OPTICAL FIBRE BIREFRINGENCE MEASUREMENT USING A PHOTO-ELASTIC MODULATOR

A. J. Barlow
Department of Electronics,
The University,
Southampton,
SO9 5NH,

Abstract

A new birefringence measurement technique for single-mode optical fibres using a photo-elastic birefringence modulator is described. The method is compared to an existing static measurement method to illustrate the sensitivity, accuracy and speed made available. Experimental results on both low-and high-birefringence fibres are presented.

The author is on leave at the Department of Electronics, University of Southampton from British Aerospace plc, Stevenage, Herts., UK.

I. Introduction

Birefringence frequently arises in single-mode optical fibres [1] and their successful application in sensors and communications relies heavily on the ability to control this property during manufacture. Coherent transmission systems [2] and fibre interferometers [3] require high-birefringence fibres [4] which can transmit a stable linear polarisation state. On the other hand ultra-low birefringence fibres [5], [6] are suited to polarimetric sensors, conventional (baseband) and coherent communications and polarisation-control devices.

The precise measurement of fibre polarisation properties therefore plays an essential role in the development of practical fibres. However, the value of linear birefringence B in a fibre can range from $B \simeq 10^{-3}$ in high-birefringence fibres [7] to $B \simeq 10^{-9}$ in low-birefringence types [6]. In high-birefringence fibres visual observation of the Rayleigh-scattering beat pattern [8] is commonly used, although this technique has a limited range and accuracy and is useful only at visible wavelengths. Another technique employing modulation of the fibre properties by stress or electromagnets is also suitable only for high-birefringence measurements [9].

The polarimetric method employing a polariser and analyser [10] is best suited to moderate and low values of birefringence, but can be adapted to measure high-birefringence by observing output polarisation variations as a function of source wavelength [11] or fibre temperature [12]. Polarimetry is a very simple method and can be used to measure both linear retardation and circular rotation, which arises from twists or the Faraday effect [6]. The basic polariser and analyser may be supplemented by a Soleil compensator or a quarter-wave plate, to improve the measurement accuracy and range. However the method becomes insensitive at low fibre retardations i.e. $<10^{o}/m$ and is far from satisfactory for the development of ultra-low birefringence fibres. In addition its performance is greatly affected by the quality of the

optical components. These inherent drawbacks arise because the birefringence to be measured is static. As is well known from ellipsometric techniques [13], modulating the birefringence dramatically improves the measurement sensitivity. In this paper the first known application of dynamic photo-elastic birefringence modulation to optical fibre measurements [14] and its use in both high and low birefringence fibre development is reported.

In Section II the performance of the static polarimetric measurement technique is evaluated theoretically and from experimental experience. It will be shown that for low-birefringence measurements, the procedure is time-consuming and the results obtained inaccurate. An appraisal of the limiting effects of optical component quality is presented.

The new photo-elastic modulation (PEM) measurement technique is described in Section III and a comprehensive analysis of the system performance presented. The experimental details of the method will also be presented. Preliminary results obtained in low and high birefringence fibres using the PEM system are presented in Section IV.

II Fibre Birefringence Measurement by Static Polarimetric Method

A) Measurement Principle

In the static polarimetric method using polariser and analyser [10], birefringence is measured by analysis of the output state of polarisation (SOP) for a given input state. Throughout this paper we will assume that the fibre of length z can be modelled in Jones Calculus form [15] as a retarder of retardation R and principal axis ϕ, followed by a circularly-birefringent element with rotation Ω. The basic apparatus is shown in Figure 1.

The polariser launches linearly-polarised light into the fibre at an azimuthal angle Θ_o. The electric vectors in x and y directions after the fibre is written in Jones Calculus form as:

$$\begin{bmatrix} E_x \\ E_y \end{bmatrix} = \begin{bmatrix} A & -B^* \\ B & A^* \end{bmatrix} \cdot \begin{bmatrix} \cos\Theta_o \\ \sin\Theta_o \end{bmatrix} E_o \qquad (1)$$

where [16]

$$A = \cos\frac{R}{2} \cdot \cos\Omega + i \sin\frac{R}{2} \cdot \cos(2\phi + \Omega) \qquad (2)$$

$$B = \cos\frac{R}{2} \cdot \sin\Omega + i \sin\frac{R}{2} \cdot \sin(2\phi + \Omega) \qquad (3)$$

and E_o is the electric field present at the polariser front face. The output from the fibre (eqn. (1)) is elliptically-polarised with an azimuthal inclination ψ given by

$$\psi = (\phi+\Omega) + \tfrac{1}{2} \tan^{-1}\left[\tan\left[2(\Theta_o-\phi)\right]\cos R\right] \qquad (4)$$

and maximum and minimum intensities I_{max} and I_{min} respectively [10]

$$I_{max} = \left[\frac{E_o^2 \cos^2\chi . \sin^2\chi . \sin^2 R}{\sin^2\chi\cos^2\gamma - \cos\chi\sin\chi\cos R\sin 2\gamma + \cos^2\chi\sin^2\gamma}\right] \qquad (5)$$

$$I_{min} = \left[\frac{1-P}{1+P}\right] \cdot I_{max} \qquad (6)$$

where

$$\chi = \Theta_o - \phi \qquad (7)$$

$$\gamma = \psi - \Omega - \phi \qquad (8)$$

and P is the polarisation of the ellipse.

$$P = \frac{I_{max} - I_{min}}{I_{max} + I_{min}} = \sqrt{1 - \sin^2 R \sin^2 2\chi} \qquad (9)$$

The output ellipse is measured using the analyser inclined at an azimuthal angle α to give an intensity I at the detector:

$$I = I_{max} \left[\left(\frac{1-P}{1+P}\right) . \sin^2(\alpha-\psi) + \cos^2(\alpha-\psi) \right] \qquad (10)$$

The fibre properties R, Ω and ϕ are now measured in a two stage process by rotating the polariser and analyser. Figure 2 shows the polarisation P [10] as a function of the relative input angle χ for various values of retardance R. When the input polariser is rotated to lie parallel to one of the fibre principal axes i.e. $\Theta_o = \phi \pm m\pi/2$, the polarisation P approaches unity i.e. a linear-polarised output occurs ($I_{min} = 0$). This "linear-input-linear-output" condition is detected as an output null (I=0) by rotating the analyser to $\alpha = \psi + \pi/2$. Having thus obtained the principal axis ϕ, the rotation is determined by the relative orientation of the analyser and polariser using eqn. (4):

$$\Omega = \alpha - \Theta_o - 90^o \qquad (11)$$

In practice, ϕ and Ω have unknown values, so the condition $\chi = 0$ is found by progressively and iteratively rotating the polariser and the analyser in turn, until the best attainable null is obtained. The retardation is then measured by rotating the polariser to give $\chi = \pi/4$. The output polarisation is now P = cosR and the ellipse azimuth is $\psi = \phi + \Omega + \pi/4$. Thus R may be obtained directly by measuring I_{min} and I_{max} using the analyser and detector. An alternative is to insert, at 'A' in Figure 1, a Soleil compensator whose axes lie parallel to those of the fibre, to enable the total system retardation to be set to zero. This condition gives a linearly-polarised output for $\chi = \pi/4$ which is detected as a null using the analyser at an angle $\alpha = \psi + \pi/2$, whereupon the fibre retardation is exactly compensated by the compensator retardation.

B) Practical Considerations

When measurements of low retardation values are carried out, $P \simeq 1$ for $\chi = \pi/4$ and hence I_{min} and I_{max} differ by several orders of magnitude (Fig. 2). The detection system must therefore have a large dynamic range. However if a Soleil compensator is used only null detection is needed throughout and the detector need not be calibrated. A second advantage of using a compensator is that the effect of source intensity or fibre launch efficiency fluctuations is reduced.

As with any fibre birefringence measurement technique the fibre must be operated within its single-mode region to prevent interference from the higher-order modes. Similarly it is important to ensure that the input and output lenses do not significantly contribute to the fibre birefringence to be measured, although compensation for their effects is possible in principle. The most important disadvantage of the static polarimetric technique is that for input angles near the principal axes $\chi \simeq 0 \pm m\pi/2$ the SOP is insensitive to changes in χ (i.e. $dP/d\chi \simeq 0$). The iteration for ϕ and Ω is therefore inherently insensitive and time-consuming, particularly at low R values where P is close to unity for all input angles.

The iteration procedure to locate ϕ and Ω was simulated by computer, to investigate the convergence of the process. Figure 3a shows the calculated minima of the relative output intensity at each intermediate polariser position and analyser position, for a series of 100 iteration cycles from the same initial polariser position, with fibre retardations of 10^{o} and 18^{o}. Note how the polariser converges asymptotically towards the principal axis ϕ (i.e. 25^{o}) as the intensity drops, while the analyser converges towards $90^{o} + \phi + \Omega$ (i.e. 115^{o}) along an essentially similar path. Figure 3b shows that the polariser approaches the principal axis exponentially with the number of iteration cycles, with a rate depending strongly on the retardation value. Clearly, at low retardation levels the iteration is prohibitively slow, while even moderate retardations require some fifty iterations to reach an offset of 5 minutes of

arc (the resolution of the rotation mounts used in the experiments to be described later). However, as the iteration proceeds, the *incremental* rotations of polariser and analyser between iteration cycles decreases, until at some point, indicated by the dashed lines in Figure 3b, these increments can no longer be resolved at the rotation mounts, so to the observer the iteration appears to have stopped. Therefore, by virtue of its asymptotic behaviour, the polarimetric measurement will always be susceptible to large experimental error in ϕ when there is finite rotation mount resolution. In addition, detector noise, shot-noise or source noise will give a practical limit of intensity resolution which further curtails the iteration procedure and increases the error in ϕ. However the subsequent error in Ω will be significantly smaller because the analyser tends to follow the polariser into the convergence. The error in ϕ will result in incorrect setting of $\chi = \pi/4$ for retardation measurement. However the retardation error will be small since $dP/d\chi \simeq 0$ at $\chi = \pi/4$ (Figure 2).

Imperfections in the components of the optical system are the primary performance limitations of the static polarimetric method and are now considered.

(i) Unpolarised light

Residual unpolarised light originates in the optics from two sources; fibre cladding modes and polariser scattering.

Cladding modes are unavoidably launched into the test fibre by the input optics and will generally be randomly polarised, so will not be rejected at the analyser. Similarly light scattered within the prism polariser will be randomly polarised and pass on to the detector, remaining unaltered by the fibre birefringence. The net effect is a background output light intensity level upon which the null must be detected.

Figure 4 shows the computed iteration for a total scattering component equal to 10^{-4} of the input intensity $I_o = |E_o|^2$, for the same fibre properties and initial polariser position as Figure 3a, curve a. As predicted the iteration proceeds

as before with an identical speed of convergence i.e. curve a, Figure 3b, but the intensity null is now superimposed on the 10^{-4} background level. The source intensity noise or vibration will cause the large background level to fluctuate, severely limiting null intensity resolution. As described before, this will give rise to errors in ϕ, Ω and R. Moreover, since the measured polarisation P will be degraded by the background light, a further error in retardation R will arise if the direct intensity measurement is used. For example a 10^{-4} scattering level will give a maximum measured P of 0.9999 and therefore a minimum measurable retardation of $\sim 1.2^{o}$.

Unpolarised light therefore behaves as an artificially-large detector noise source in the measurements, and should be reduced as much as possible by carefully index-matching the fibre and by careful choice of polarising components.

(ii) Polariser leakage

In practice, finite amounts of the undesired polarisation are transmitted by the polariser and analyser. At the fibre input, the Jones matrix expression would be

$$\begin{bmatrix} E_x \\ E_y \end{bmatrix}_{\text{INPUT}} = \begin{bmatrix} \cos\theta_o & -\sin\theta_o \\ \sin\theta_o & \cos\theta_o \end{bmatrix} \begin{bmatrix} p_1 & 0 \\ 0 & p_2 \end{bmatrix} \begin{bmatrix} 1 \\ 1 \end{bmatrix} E_o \qquad (12)$$

where the source is assumed to be unpolarised, p_1 and p_2 are the transmission of the polariser in the desired and undesired directions respectively. Since the resultant of two linearly-polarised beams is also linearly-polarised we may write:

$$\begin{bmatrix} E_x \\ E_y \end{bmatrix}_{\text{INPUT}} = \begin{bmatrix} \cos\theta' \\ \sin\theta' \end{bmatrix} \cdot p' \qquad (13)$$

where Θ' is the true input angle and p' is the net transmission of the polariser:

$$\Theta' = \tan^{-1}\left[\frac{p_1 \sin\Theta_o + p_2 \cos\Theta_o}{p_1 \cos\Theta_o - p_2 \sin\Theta_o}\right] \qquad (14)$$

and

$$p' = \sqrt{p_1^2 + p_2^2} \qquad (15)$$

Thus leakage simply gives rise to systematic offset of the resultant input direction $\Theta' - \Theta_o$ and measurement of fibre birefringence may be performed as before but noting that Θ' replaces Θ_o in eqns. (1) to (11).

For good quality polarisers p_2/p_1 approaches 10^{-3} [17] giving an offset $|\Theta' - \Theta_o| \simeq$ 6 mins of arc, a negligible error in ϕ.

At the fibre output, leakage will allow a small amount of I_{max} will reach the detector when the analyser is aligned for I_{min} and vice versa. The output intensity (eqn. (10)) is now:

$$I = I_{max}\left[\left(\frac{1-P}{1+P}\right)\left(k_1\sin^2(\alpha-\psi) + k_2\cos^2(\alpha-\psi)\right) + k_1\cos^2(\alpha-\psi) + k_2\sin^2(\alpha-\psi)\right] \qquad (16)$$

where $k_1 = p_1^2$ and $k_2 = p_2^2$.

The computer iteration results are shown in Figure 5a for $p_2/p_1 = 1.88 \times 10^{-3}$ and in Fig. 5b for $p_2/p_1 = 1.9 \times 10^{-2}$, using the fibre parameters of Figure 3a, curve a. Polariser leakage gives rise to a background level which, unlike that due to scattering, varies with polariser and analyser positions. Thus the sensitivity of each intermediate polariser and analyser iteration, $dI/d\chi$ and $dI/d\alpha$ respectively are reduced, but the speed of convergence of the overall procedure is unaltered. But the presence of a background level will give rise to error in ϕ, Ω and R due to noise and vibration as for unpolarised light.

III Fibre Birefringence Measurements Using a Photo-Elastic Modulator

A) The Photo-Elastic Modulator

As already demonstrated, measurement of a static birefringence cannot be accomplished with satisfactory accuracy and sensitivity. Dramatic improvements in measurement sensitivity may be obtained by dynamically modulating the birefringence under test [9]. Such a technique is frequently applied to automatic ellipsometers [13], [18] by using a photo-elastic modulator (PEM). The device is easily adapted for use in fibre birefringence measurements.

The photo-elastic modulator [19] consists of a fused silica optical element in which an oscillating strain-birefringence is set up by a resonant acoustic wave produced by a piezo-electric quartz crystal transducer. The transducer itself forms part of a crystal oscillator circuit used to drive the device. The silica element behaves as a retardation plate whose retardation varies sinusoidally with time. The element vibrates on rubber mounts causing the light beam to wander, so it is necessary to place the PEM after the test fibre to avoid fibre launch efficiency fluctuations.

B) Theory and Measurement Principle

The basic experimental arangement used is shown in Figure 6. Close similarities with existing ellipsometric methods [18], [13] using a PEM will be observed with the exception that in this case the polariser and modulator/analyser assembly may be rotated to line up with the unknown principal axes directions. Linearly-polarised light of intensity I_o is launched into the fibre with an azimuthal inclination of θ_o to the fibre axes, using a prism polariser. Note that for convenience the principal axis direction ϕ is taken as the reference direction (i.e. $\phi \equiv 0$) The modulator and prism analyser rotate as one assembly with a fixed angle of 45^o relative to each other, and are inclined at an angle r. The Jones calculus equation is written

$$\begin{bmatrix} E_x \\ E_y \end{bmatrix} = [A][B] \cdot \begin{bmatrix} \cos\Omega & -\sin\Omega \\ \sin\Omega & \cos\Omega \end{bmatrix} \cdot \begin{bmatrix} e^{\frac{iR}{2}} & 0 \\ 0 & e^{\frac{-iR}{2}} \end{bmatrix} \cdot \begin{bmatrix} \cos\theta_o \\ \sin\theta_o \end{bmatrix} \cdot \sqrt{I_o} \qquad (17)$$

where

$$[A] = \begin{bmatrix} \cos^2 (r-45) & \cos(r-45).\sin(r-45) \\ \cos(r-45).\sin(r-45) & \sin^2(r-45) \end{bmatrix} \qquad (18)$$

represents the analyser and

$$[B] = \begin{bmatrix} \cos^2 r.\ e^{\frac{i\delta}{2}} + \sin^2 r.e^{\frac{-i\delta}{2}} & 2i\cos r.\sin r.\sin\frac{\delta}{2} \\ 2i\cos r.\sin r.\sin\frac{\delta}{2} & \cos^2 r.e^{\frac{-i\delta}{2}} + \sin^2 r.e^{\frac{i\delta}{2}} \end{bmatrix} \qquad (19)$$

represents the modulator. The modulator retardation δ is given by

$$\delta(t) = K \sin \omega t \qquad (20)$$

where K is the modulation amplitude, which may be set to any aribtrary value and $\omega = 2\pi f$, f being the modulator drive frequency (50KHz). Simplifying Equation (17) gives the light intensity $I = |E_x|^2 + |E_y|^2$ at the photo-detector

$$I = \frac{I_o}{2} \cdot \begin{bmatrix} 1 + \sin R.\sin\delta.\sin 2\theta_o + \cos\delta.\ \cos 2\theta_o.\sin(2r-2\Omega) \\ - \cos R.\sin 2\theta_o.\cos(2r-2\Omega).\ \cos\delta \end{bmatrix} \qquad (21)$$

Harmonic analysis of $\sin\delta$ and $\cos\delta$ yields the intensity modulation component at frequency W, W_1, and that at frequency 2W, W_2:

$$W_1 = I_o.J_1(K).\sin R.\sin 2\theta_o \qquad (22)$$

$$W_2 = I_o.J_2(K).\left[\cos 2\theta_o.\sin(2r-2\Omega) - \cos R.\sin 2\theta_o.\cos(2r-2\Omega)\right] \qquad (23)$$

where J_1 and J_2 are first and second-order Bessel functions of the first kind respectively. W_1 and W_2 are measured using phase-sensitive detectors operating at f and 2f respectively. The sensitivity S_1 of the fundamental frequency component W_1 to a rotation of the input polariser is

$$S_1 = \frac{dW_1}{d\theta_o} \propto \sin R \cos 2\theta_o \qquad (24)$$

and for the second-harmonic signal W_2 the sensitivity S_2 to input polariser position is

$$S_2 = \frac{dW_2}{d\theta_o} \propto \left[\sin 2\theta_o \sin(2r-2\Omega) - \cos R \cos 2\theta_o \cos(2r-2\Omega)\right] \qquad (25)$$

Similarly, the sensitivities T_1 and T_2 of the fundamental and second-harmonic signals to modulator position are

$$T_1 = \frac{dW_1}{d(r-\Omega)} = 0 \qquad (26)$$

$$T_2 = \frac{dW_2}{d(r-\Omega)} \propto \left[\cos 2\theta_o \cos(2r-2\Omega) + \cos R \sin 2\theta_o \sin(2r-2\Omega)\right] \qquad (27)$$

The measurement proceeds as follows. The input polariser is rotated until the fundamental signal W_1 is zero. Since T_1 is zero, this procedure may be performed for any initial modulator position. As W_1 approaches zero, the input polariser becomes aligned to the principal axis direction i.e. $\theta_o \to 0$. Here the sensitivity of the rotation procedure is greatest and proportional to sinR. Thus the principal axis may be easily found even for small values of R if sufficient signal gain is used. Having determined the principal axis in this manner, the rotation Ω is obtained by retaining the input polariser position $\theta_o = 0$ and rotating the modulator/analyser until W_2 is also zero. In this condition W_1 remains zero, and the modulator is aligned to the rotated output linear polarisation plane. The sensitivity T_2 of the procedure reaches a maximum at this point, so that the correct modulator position may be accurately found and the rotation calculated from the relative modulator and input polariser azimuths.

The input polariser now rotated by 45^{o} while the modulator azimuth is left unchanged. In this condition $W_1 \propto \sin R$ and $W_2 \propto \cos R$, so ratiometric detection detection of W_1/W_2 gives a calibrated output proportional to tanR, independent of the source intensity or fibre launch efficiency. Note that the sign of R with respect to the principal axis measured above is given. Another advantage is that the sensitivities S_1, S_2, T_2, T_1 all become close to zero, so that slight misalignments of polariser and modulator have negligible effect on the measurement of R itself. An alternative method is to use a Soleil compensator to null R, giving zero total system retardation and hence a zero W_1 signal. This retains a degree of independence from source intensity variations while increasing the measurement dynamic range. Since W_2 is no longer of concern, the signal gain may be greatly increased to improve the detection of a zero in W_1.

It is important to note that in this method R, Ω and ϕ are determinable with potentially high sensitivity simply by detecting respective zeros in W_1 and W_2, and most significantly, without using a time-consuming iteration procedure. The method is therefore expected to be extremely fast, sensitive and accurate in practice and particularly attractive for measurement of small retardation values.

C) Detection System

The basic detection system using a c.w. source is shown in Figure 7. The photo-diode signal is amplified to provide sensitive zero detection in the 50KHz and 100KHz channels. In the case of the 50KHz channel, a 40dB-gain 3Hz-bandwidth coherent tracking filter blocks the large W_2 signal obtained when measuring retardation using the compensator to prevent PSD input overload. The lock-in amplifier operates in "2f" mode with a sensitivity similar to that of the 50KHz channel. A 50KHz reference signal is derived from the modulator controller. The ratiometer and voltmeter provide source intensity compensation.

D) Sources of Error

In common with the static measurement method of Section II, the test fibre must be operated in its single-mode region, while the input and output lenses must have minimal birefringence. An inherent and important advantage of the PEM technique described is its ability to discriminate

between unpolarised and polarised light emerging from the fibre. The unpolarised light caused by input polariser scattering or cladding modes remains unaltered by birefringence modulation and therefore produces a d.c. light level after the analyser. Only the polarised light emerging from the fibre mode undergoes modulation. Thus by ignoring the d.c. intensity component and using only the modulated signals W_1 and W_2 to measure birefringence, the PEM method described achieves almost complete immunity from unpolarised light. Scattering of the polarised light at the analyser into other polarisation states will produce a slight reduction in output sensitivity. The PEM method is therefore particularly easy to use with fibres with matched or raised-index claddings where perfect cladding mode-stripping is not possible.

As shown in Section IIB, orthogonal polarisation leakage in the input polariser produces only a small systematic error in the apparent input polarisation azimuth. On the other hand, residual orthogonal polarisation leakage at the analyser represents a second independent low-intensity light path through the PEM system, with the analyser azimuth orthogonal to the principal transmission direction considered in Figure 6. Analysis by Jones Calculus yields new W_1 and W_2 components of the same form as those of eqns. (22) and (23) but with opposite signs. Thus, for a primary analyser amplitude transmission of p_1 and a leakage of p_2, the total output signals W_1 and W_2 are given by eqns. (22) and (23) with pre-multiplication factors of $\left[p_1^2 - p_2^2\right]$. Since $p_1 >> p_2$ in virtually all polarisers, this is a negligible change in output sensitivity.

Another source of potential error is the residual strain-birefringence in the PEM, which arises primarily from the static pressure of the rubber mounts used to grip the modulator crystal assembly. The magnitude of the residual birefringence varies across the modulator aperture and with modulator orientation. Fortunately the latter effect is reduced by operating the modulator on the vertical bench, while collimating the fibre output ensures that only a small

central area of the modulator element is used. A typical value for the stress-birefringence δ' is $\sim 0.5^{o}$.

The effect of δ' may be analysed as follows. In eqn. (20), $\delta(t)$ is now written as:

$$\delta(t) = \delta' + K \sin \omega t \tag{28}$$

Harmonic analysis of $\cos \delta(t)$ and $\sin \delta(t)$ in eqn. (21) is performed by first decomposing $\delta(t)$:

$$\cos \delta(t) = \cos\delta'.\cos(K\sin\omega t) - \sin\delta'.\sin(K\sin\omega t) \tag{29}$$

$$\sin \delta(t) = \sin\delta'.\cos(K\sin\omega t) + \cos\delta'.\sin(K\sin\omega t) \tag{30}$$

Immediately it becomes obvious that cross-modulation of the original W_1 and W_2 signals (eqns. (22) and (23)) occurs and the rotations of input polariser and modulator to measure ϕ, Ω and R will be subject to offsets. The new signals W_1 and W_2 become:

$$W_1 = I_o.J_1(k)\Big\{ \sin R.\sin 2\theta_o.\cos\delta' - \sin\delta' \Big[\cos 2\theta_o.\sin(2r-2\Omega) - \cos R.\sin 2\theta_o.\cos(2r-2\Omega$$

(31)

$$W_2 = I_o.J_2(k)\Big\{ \cos\delta' \Big[\cos 2\theta_o.\sin(2r-2\Omega) - \cos R.\sin 2\theta_o.\cos(2r-2\Omega + \sin\delta'.\sin R.\sin 2\theta_o \Big\}$$

(32)

The offset terms containing $\sin\delta'$ reduce to zero at $\theta_o = 0$, $r-\Omega = 0$. Therefore the correct principal axis and rotation may be found providing the rotations of polariser and modulator/analyser are iterated until both W_1 and W_2 are simultaneously zero. However when $\theta_o = 45^{o}$, $r - \Omega = 0$ for the measurement of retardation R the ratio $\frac{W_1}{W_2} \propto \tan(\delta' + R)$. Thus δ' introduces an offset which is significant when ultra-low birefringence fibres are under test. Moreover, in such cases, the iteration to determine ϕ and Ω is slow.

To confirm the effect of δ' experimentally, the modulator was set up with no fibre in place i.e. $R = 0$, $\Omega = 0$, $\phi = 0$. In this case the output $W_1/W_2 = \tan \delta'$ for $\theta_o = 45^o$. By measuring the residual 50KHz signal, δ' was found to be about $+ 0.5^o$ with the fast axis parallel to the $\theta_o = 0$ direction in Figure 6. Next, a Soleil compensator was inserted and the measurement of its retardation at various compensator settings carried out as described in Section IIIB. For each iteration cycle W_1 was first zeroed by rotating the input polariser. The modulator was then rotated to zero W_2, whereupon W_1 moves to a non-zero value. The polariser and modulator positions are then noted before a second iteration is performed. Iterations were stopped when the change in polariser and analyser positions between successive iterations was equal to or less than the resolution limit of the rotation mounts (0.08^o). The number of iterations required for various values of R using the compensator is shown in Figure 8. Also shown is the result of a computer iteration to the same precision using eqns. (31) and (32) showing very close agreement. The actual polariser and modulator positions for each intermediate iteration step predicted by the computer showed a similarly close agreement with those recorded in the experiments. Note that at very low values of R the convergence slows so that the successive polariser and modulator rotations are smaller than the angular resolution specified. Moreover if δ' and R have opposite signs and R is small the iteration no longer reaches the principal axis condition of $\theta_o = 0$, $r = \Omega$. Figure 9 shows the regions of correct convergence for various R and δ' values.

For moderate retardation values the number of iterations required to reach resolution limit is only two or three. Figure 3b compares the convergence of the PEM method (curve d) and the static polarimetric method of Section II (curve a), for a fibre retardation of 18^o, and the same initial offset for polariser and/or analyser/modulator. Note how the PEM method converges rapidly to give resolution limit after only two iteration cycles.

To recap, δ' reduces the speed of the measurement technique, but provided R exceeds δ' by at least a factor of two, the only error incurred is in the value of R which will be offset by an amount δ'. If the sample has zero linear birefringence, the outputs are

$$W_1 = \sin\delta' . \sin(2r - 2\Omega - 2\theta_o) \quad (33)$$

$$W_2 = \cos\delta' . \sin(2r - 2\Omega - 2\theta_o) \quad (34)$$

and therefore, δ' only marginally reduces the sensitivity of rotation measurement using a zero in W_2. Nevertheless, it is advantageous to simply compensate δ' to remove the necessity for iteration and to improve the measurement accuracy for low retardation levels. This is done, by inserting into the rotating modulator assembly, a variable retardation plate consisting of a thin glass plate pressurised at its edges by a screw, to induce a stress-birefringence δ''. Exact compensation of δ' is indicated by a zero in the W_1 signal when the test fibre is removed (eqn. (33)) and the polariser is inclined at 45^o to the modulator axes. This procedure is repeated before each new fibre measurement, to compensate for variations of δ'.

The lowest fibre retardation measurable is limited by the finite birefringence of the lenses. However the measurement sensitivity per se is far higher, limited only by photo-diode shot-noise and laser source polarisation noise occuring within the pass-band of the detection system. Laser noise arises from inter-mode beating in the laser cavity and in the randomly-polarised He-Ne laser used in experiments was at a level equal to the maximum 50KHz signal level for retardations of 0.1^o or less. However for moderate R values resolution in R, ϕ and Ω is better than the mechanical resolution of the optical equipment. A single-frequency laser source would greatly enhance the present performance.

IV Experimental Results

A) Low-Birefringence Fibre Measurements

Fibre spinning (twisting a fibre during drawing) is nowawell-established technique [6] for the routine production of ultra-low birefringence fibres from birefringent fibre preform rods. The fibre local anisotropy is averaged by a rapid frozen-in 'spin' to give a residual overall anisotropy

of around 1^{o} or less. These levels of retardation are in practical instances negligible, but may be measured using the PEM technique described. The results of a measurement of the residual birefringence of ~1 metre of spun fibre as a function of ambient temperature using the ratio output W_1/W_2 is shown in Figure 10. Note that the output retardation level is mainly due to the lenses. However negligible change in the measured retardation occurs with increase in temperature, indicating that the residual anisotropy of the spun fibre is negligible at all temperatures. Note that a direct linear retardation readout is obtained, indicating that long-term stability tests are extremely simple with the PEM technique. Figure 10 verifies that a spun fibre may be considered "polarisation-transparent" over a wide temperature range - an important property which may be exploited in the design of controlled fibre-birefringence devices such as waveplates, filters and isolators [20].

The PEM technique is also ideal for examination of the long-term drifts of fibres with moderate birefringence, by first compensating the retardation at a particular time using a Soleil compensator. Any subsequent deviations in retardation with time, temperature etc. from this reference level are recorded simply as a linear change in output W_1/W_2.

B) High-Birefringence Fibre Measurements

Although the PEM technique is ideal, and indeed essential, for low birefringence measurements, it is also useful in measurements on high-birefringence fibres, where, for example, it can be used to determine very small changes due to temperature or aging.

In a fibre length with several tens or hundreds of 2π beat lengths the output SOP will undergo cyclic changes as the total retardation passes through multiples of 2π with changes in temperature, but will not reflect the sense of birefringence change. In contrast, the PEM can be used

to observe the retardation changes directly and furthermore quadrature outputs $W_1 \propto \sin R$ and $W_2 \propto \cos R$ are available. This allows complex birefringence hysteresis effects caused by, for example, thermally-induced glass volume changes [21] to be observed unambiguously. Figure 11a shows the 50KHz and 100KHz signals obtained [21] in a high-birefringence "bow-tie" fibre [7] as a function of increasing fibre temperature. Note the abrupt change in phase in the 50KHz (sinR) curve at $\sim 450^{\circ}C$. Figure 11b is the beat length variation with temperature computed from Figure 11a. Also shown is the slow-cooling characteristic. The interpretation of this curve is given elsewhere [21].

Similar "beat-counting" techniques could be used to observe the birefringence of a high-birefringence fibre as a function of wavelength [11]. Again the quadrature retardation outputs allow unambiguous determination of complex birefringence changes, but to maintain a constant amplitude of birefringence modulation, the modulator drive must be changed linearly with wavelength [19]. A simpler alternative is to observe the zero-crossings of the sinR and cosR outputs which gives extremely accurate points on the dispersion curve for birefringence. Note that the PEM technique will give four points for each 2π of retardation change while observation of the output SOP gives only one. Hence much more detailed and accurate dispersion measurements may be obtained by the PEM method.

V Conclusion

In this paper the first known application of photo-elastic birefringence modulation (PEM) to the measurement of optical fibre polarisation properties is described. A modulation method has been developed which has a resolution for principal axis, retardation and rotation of at least 0.1° and is simple, fast and very sensitive even at very low retardation levels. A comparison with the static polarimetry technique previously used for fibres reveals that the latter method is insensitive, time-consuming, inaccurate and severely performance-limited by the quality of the polarisers and analysers used. In contrast, the PEM modulator technique is

tolerant to polariser quality and to fibre cladding modes and remains sensitive even at low retardation levels. The lowest retardation measurable is limited only by lens birefringence , shot-noise and source noise. In addition, quadrature retardation outputs are available, allowing both the sign of birefringence and complex birefringence changes with temperature and wavelength to be determined.

Experimental results have been presented illustrating the versatility and accuracy of the method.

In conclusion, the PEM method is ideal for fibre birefringence measurements and provides sensitive and accurate results very simply and quickly over a range of birefringence encountered in optical fibres.

Acknowledgements

The author thanks A. Ourmazd for providing the high-birefringence measurement results, E.J. Tarbox, R.D. Birch and R.J. Mansfield for supplying fibre samples and D.N. Payne and M.P. Varnham for helpful discussions.

References

1. D.N. Payne, A.J. Barlow, J.J. Ramskov Hansen,: "Development of low and high birefringence optical fibres", IEEE J. Quantum Electron., QE-18, 1982, pp. 477-487.

2. Y. Yamamoto and T. Kimura,: "Coherent optical fibre transmission systems", IEEE J. Quantum Electron., QE-17, 1981, pp. 919-935.

3. T.G. Giallorenzi et al.: "Optical fibre sensor technology", IEEE J. Quantum Electron., QE-18, 1982, pp. 626-665.

4. V. Ramaswamy, W.G. French, and R.D. Standley: "Polarisation characterstics of non-circular core single-mode fibres", Appl. Optics, 17, 1978, pp. 3014-3017.

5. S.R. Norman, D.N. Payne, M.J. Adams and A.M. Smith: "Fabrication of single-mode fibres exhibiting extremely low polarisation birefringence", Electron. Lett., 15, 1979, pp. 309-311.

6. A.J. Barlow, D.N. Payne, M.R. Hadley and R.J. Mansfield: "Production of single-mode fibres with negligible intrinsic birefringence and polarisation mode dispersion", Electron. Lett., 17, 1981, pp. 725-726.

7. R.D. Birch, D.N. Payne, M.P. Varnham: "Fabrication of polarisation-maintaining fibres using gas phase etching", Electron. Lett., 18, 1982, pp. 1036-1037.

8. I. P. Kaminow: "Polarisation in optical fibres", IEEE J. Quantum Electron., QE-17, 1981, pp. 15-22.

9. A. Simon and R. Ulrich: "Evolution of polarisation along a single-mode fibre", Appl. Phys. Lett., 31, 1977, pp. 517-520.

10. A. Papp and H. Harms: "Polarisation optics of index-gradient optical waveguide fibres", Appl. Optics, 14, 1975, pp. 2406-2411.

11. S.C. Rashleigh and M.J. Marrone: "Polarisation holding in elliptical-core birefringent fibres", IEEE J. Quantum Electron., QE-18, 1982, pp. 1515-1523.

12. K. Mochizuki, Y. Namihara, Y. Ejiri: "Birefringence variation with temperature in elliptically cladded single-mode fibres", Appl. Optics, 21, 1982, pp. 4223-4228.

13. R.M.A. Azzam and N.M. Bashara: "Ellipsometry and polarised light", North Holland, 1977.

14. A.J. Barlow and D.N. Payne: "Measurement of fibre polarisation properties using a photo-elastic modulator", Symposium on Optical Fibre Measurements, Boulder, Colorado, USA, October 1982.

15. R.C. Jones: "A new calculus for the treatment of optical systems", Part I-III, J. Opt. Soc. Amer. 31, 1941, pp. 488-503.

16. F.D. Kapron, N.F. Borrelli and D.B. Keck: "Birefringence in dielectric optical waveguides", IEEE J. Quantum. Electron., 8, 1972, pp. 222-225.

17. W.A. Shurcliff, "Polarised Light", Oxford, 1962.

18. S.N. Jasperson and S.E. Schnatterly: "An improved method for high reflectivity ellipsometry based on a new polarisation modulation technique", Rev. Sci. Inst., 40, 1969, pp. 761-767.

19. Hinds International Inc., Portland, Oregon, USA.

20. G.W. Day, D.N. Payne, A.J. Barlow and J.J. Ramskov Hansen: "Faraday rotation in coiled monomode optical fibres: isolators, filters and magnetic sensors", Optics Lett., 7, 1982, pp. 238-240.

21. A. Ourmazd, R.D. Birch, M.P. Varnham, D. N. Payne and E.J. Tarbox, "Enhancement of birefringence in polarisation-maintaining fibre by thermal annealing", Electron. Lett., 19, 1983, pp. 143-144.

Figure Captions

Figure 1 Optical arrangement for measurement of birefringence by static polarimetric method. Input and output lenses have been omitted for clarity.

Figure 2 Polarisation P of the output ellipse from a fibre with retardation values shown, as a function of input polariser angle χ.

Figure 3 Computer simulation of the static polarimetric method :

(a) Relative output intensity at each minimum for 100 successive iteration cycles plotted against the intermediate polariser and analyser positions. Initial polariser position = 38°, fibre rotation = 0°, principal axis = 25°. Curves a) for retardation = 18°, curves b) for retardation = 10°.

(b) Input polariser offset χ as a function of iteration number for fibre retardation of a) 18°, b) 10°, c) 5°. Principal axis = 25°, rotation = 0°, initial polariser position = 38°. Curve d) is the offset calculated for the PEM technique of Section III with residual stress birefringence $\delta' = 0.5^{\circ}$.

Figure 4 Computer simulation of the static polarimetric measurement technique showing the relative output intensity minima at each intermediate polariser and analyser position for 100 successive iteration cycles with scattered light level = 10^{-4}. Initial polariser position = 38°, principal axis = 25°, rotation = 0°, retardation = 18°.

Figure 5 Computer simulation of the static polarimetric technique for finite polariser leakage showing relative output intensity minima at polariser and analyser position for 100 successive iteration

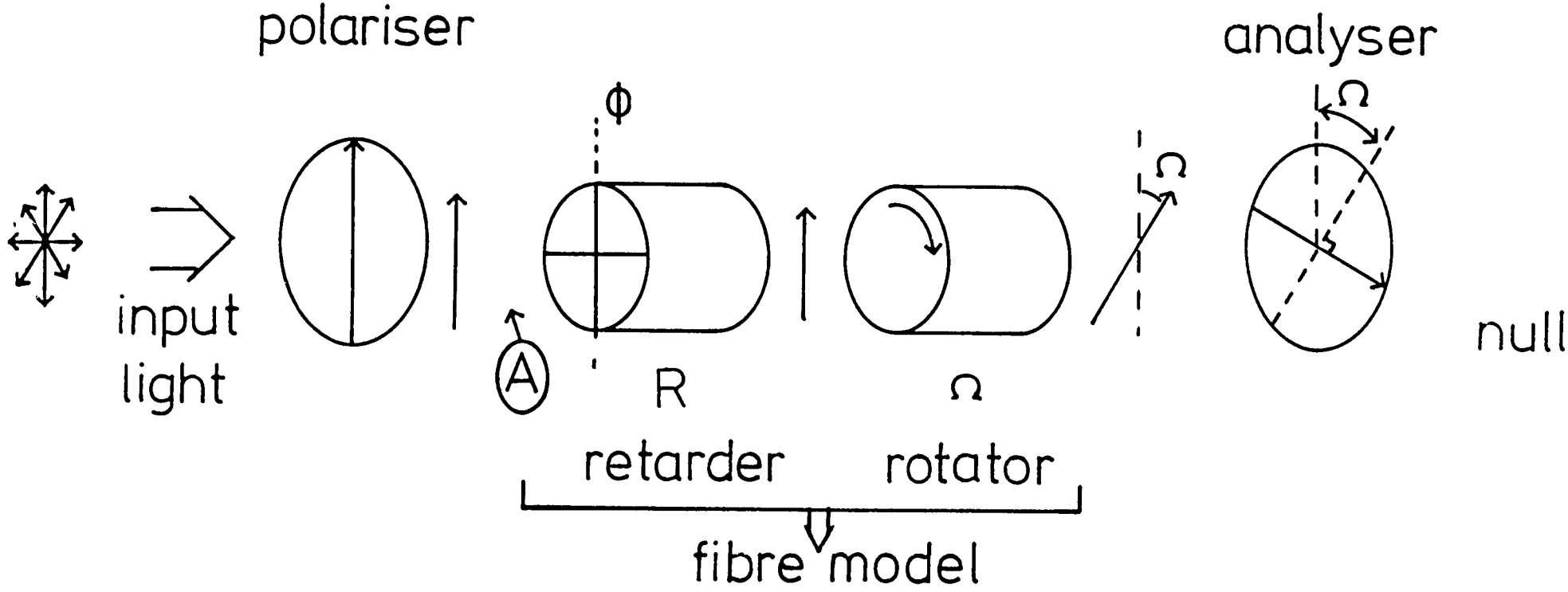
polariser
analyser
Φ
Ω
Ω
input
light
A
R
Ω
null
retarder
rotator
fibre model

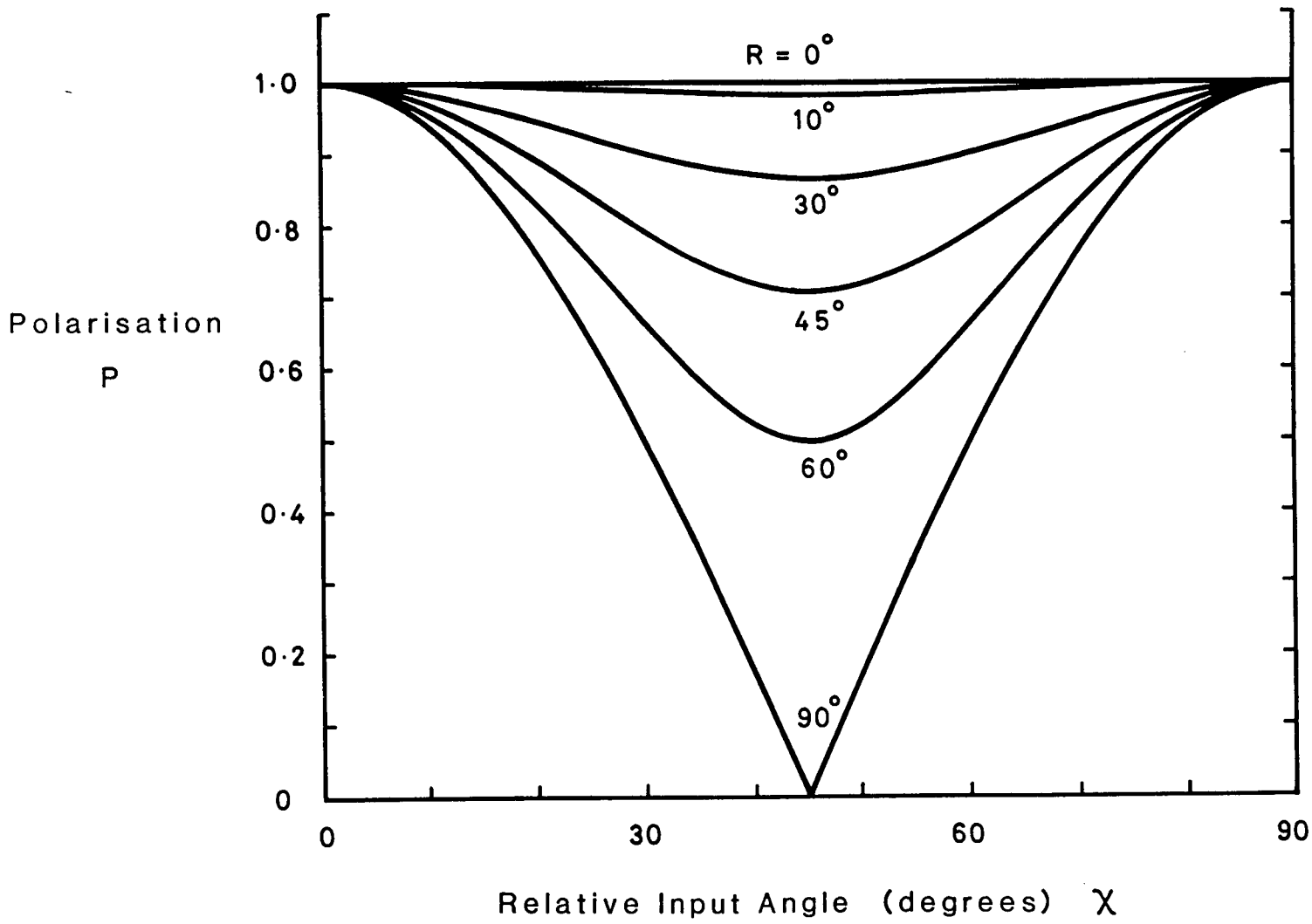
R = 0°
10°
30°
45°
60°
90°
1·0
0·8
0·6
0·4
0·2
0
Polarisation
P
0
30
60
90
Relative Input Angle (degrees) χ

fig. 2

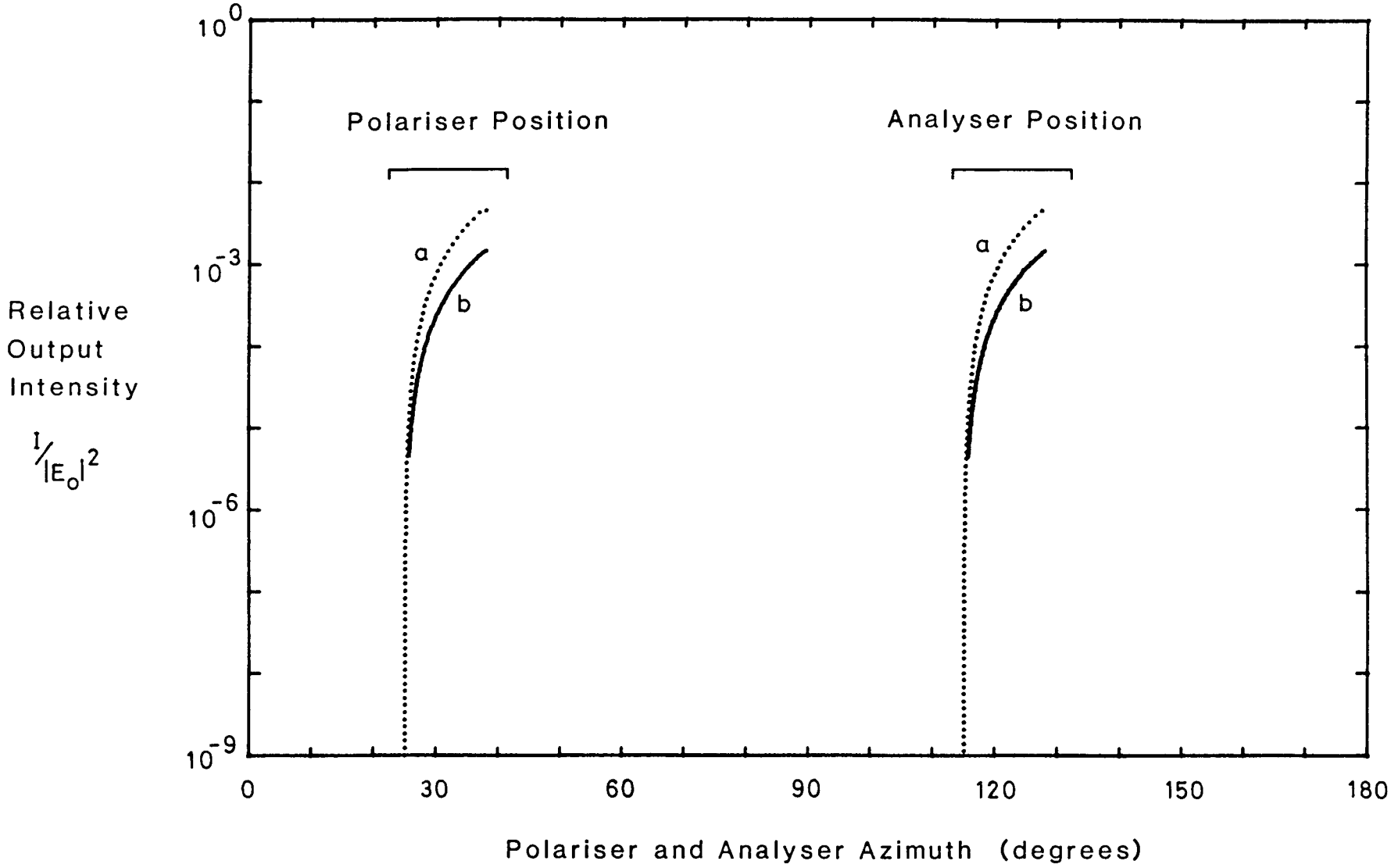
Relative
Output
Intensity
I/|E0|2
10^0
10^-3
10^-6
10^-9
Polariser Position
Analyser Position
a
b
a
b
0
30
60
90
120
150
180
Polariser and Analyser Azimuth (degrees)

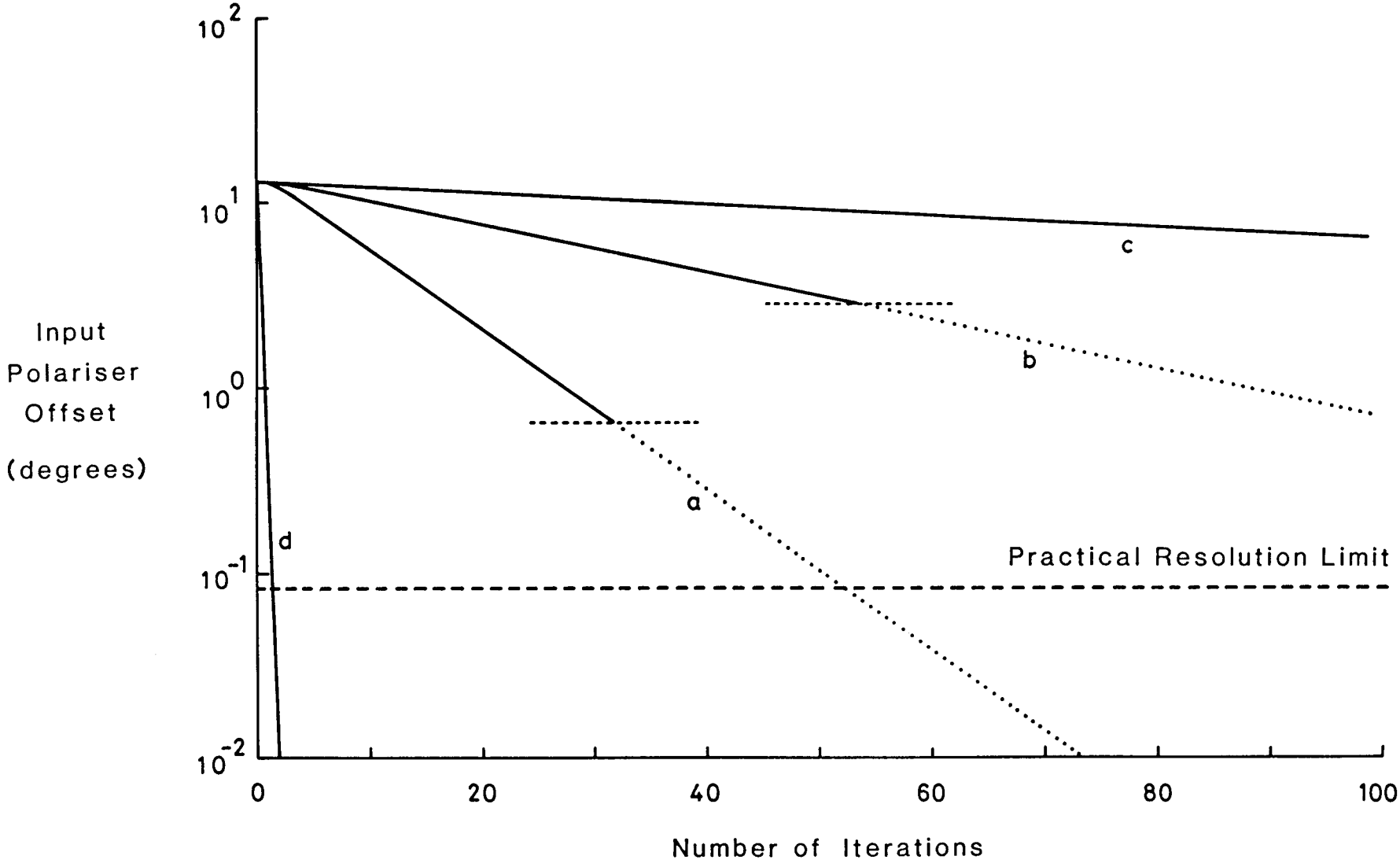
Input
Polariser
Offset
(degrees)
10^2
10^1
10^0
10^{-1}
10^{-2}
a
b
c
d
Practical Resolution Limit
0
20
40
60
80
100
Number of Iterations

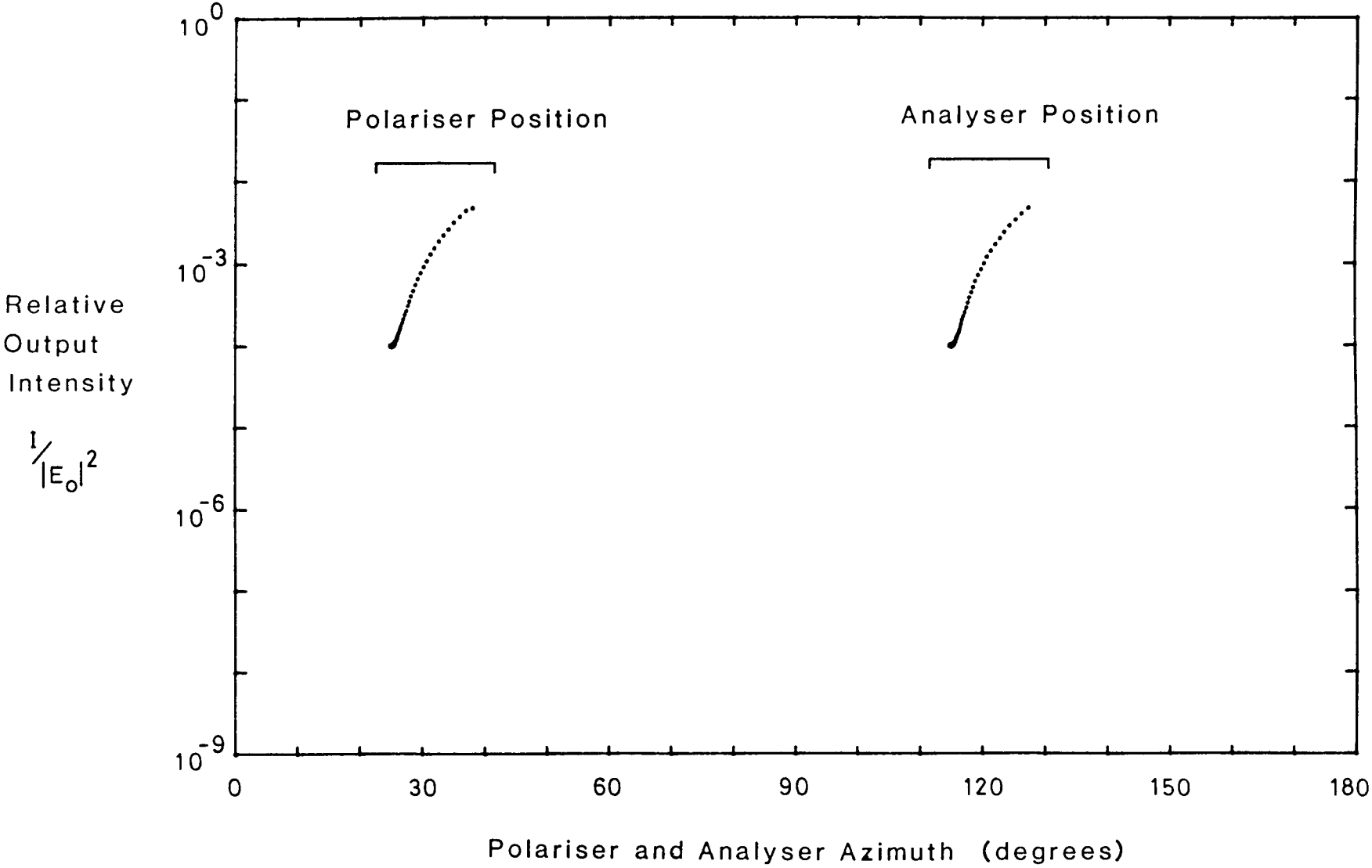
Polariser Position
Analyser Position
Relative Output Intensity
I/|E_o|^2
10^0
10^-3
10^-6
10^-9
0
30
60
90
120
150
180
Polariser and Analyser Azimuth (degrees)

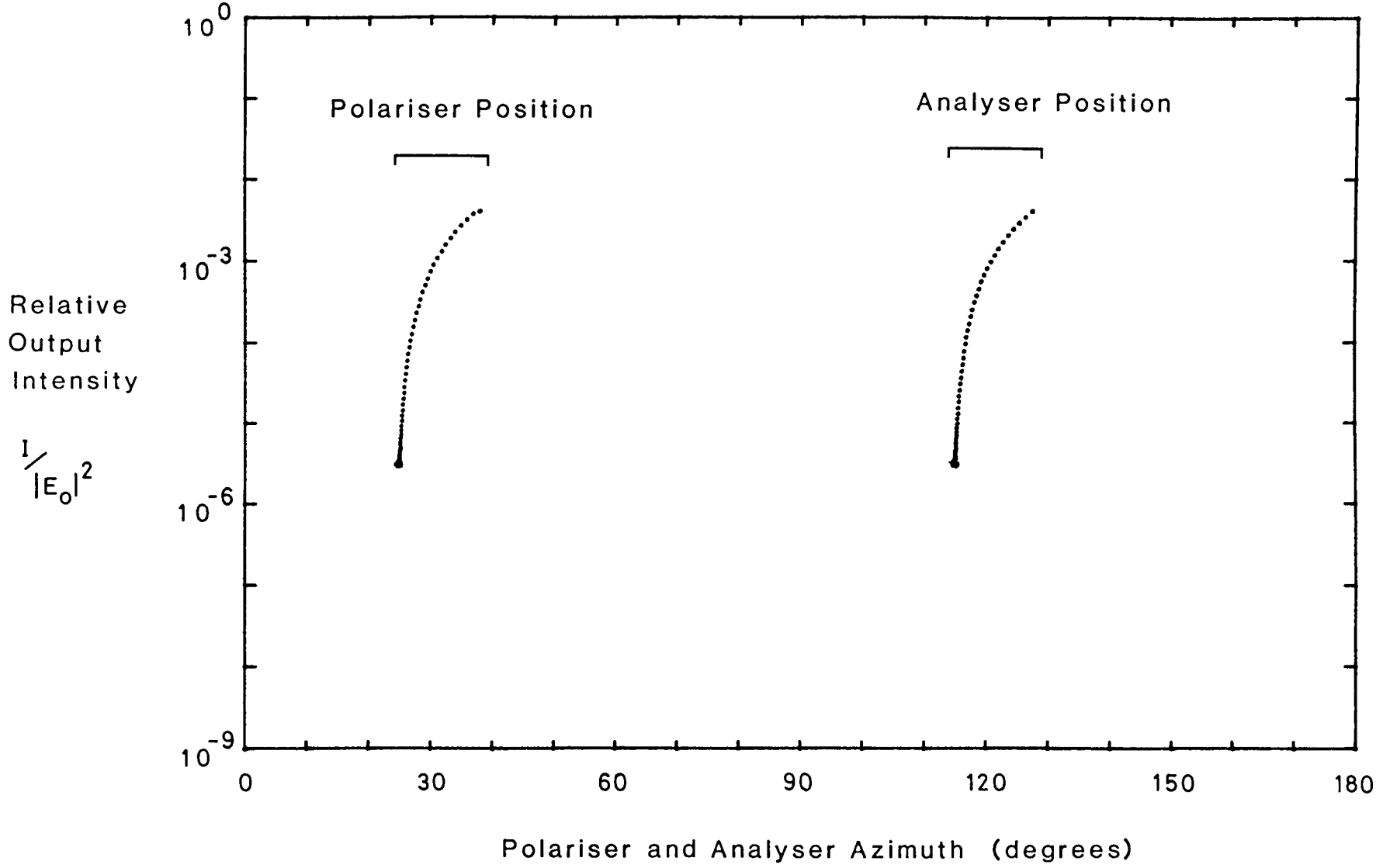
Polariser Position
Analyser Position
10^{0}
10^{-3}
10^{-6}
10^{-9}
Relative Output Intensity
$I/|E_o|^2$
0
30
60
90
120
150
180
Polariser and Analyser Azimuth (degrees)

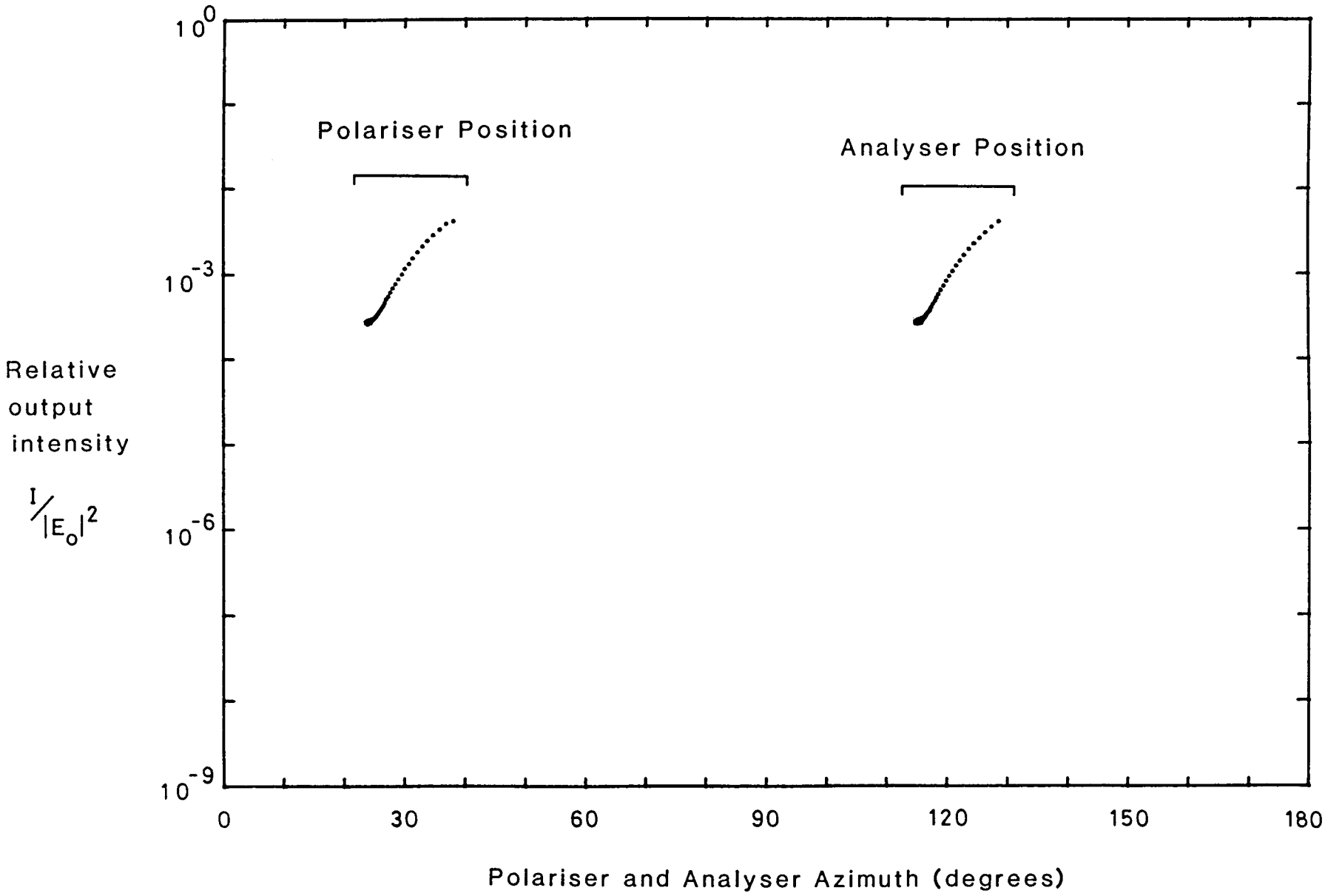
10^0
10^{-3}
10^{-6}
10^{-9}
Polariser Position
Analyser Position
Relative output intensity
$I/|E_o|^2$
0
30
60
90
120
150
180
Polariser and Analyser Azimuth (degrees)

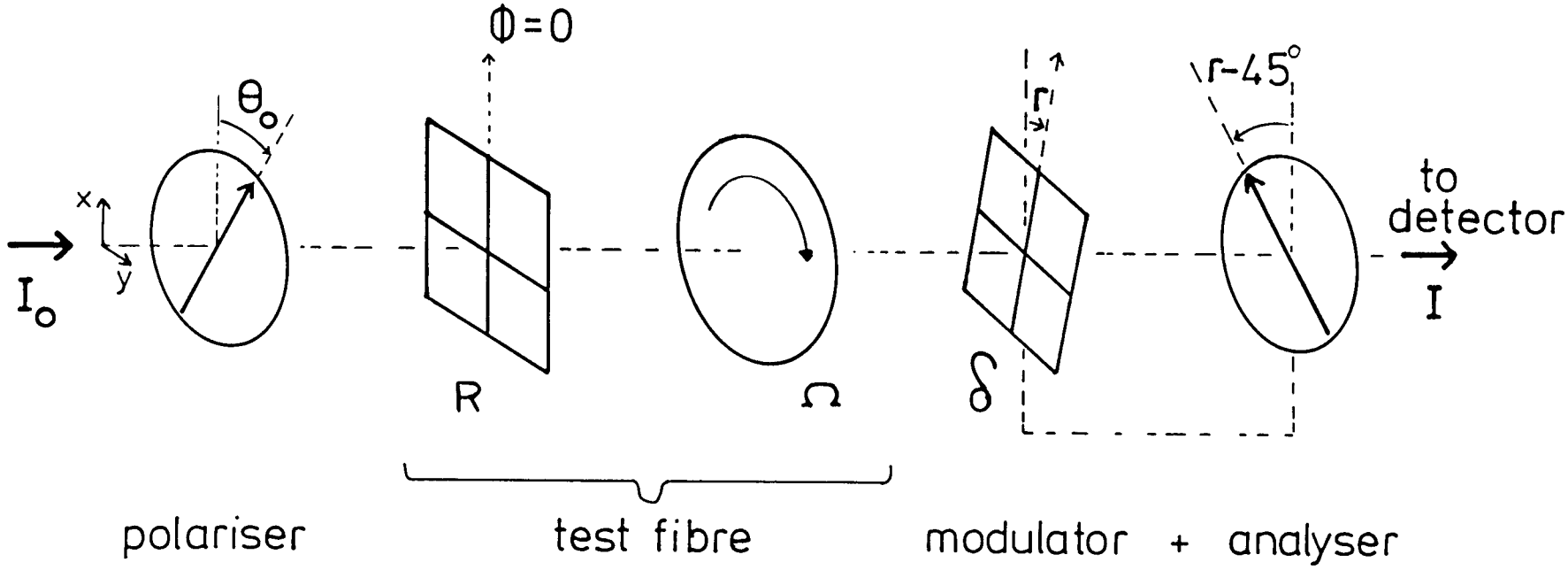
Φ=0
θo
x
y
Io
R
Ω
δ
r
r-45°
to
detector
I
polariser
test fibre
modulator + analyser

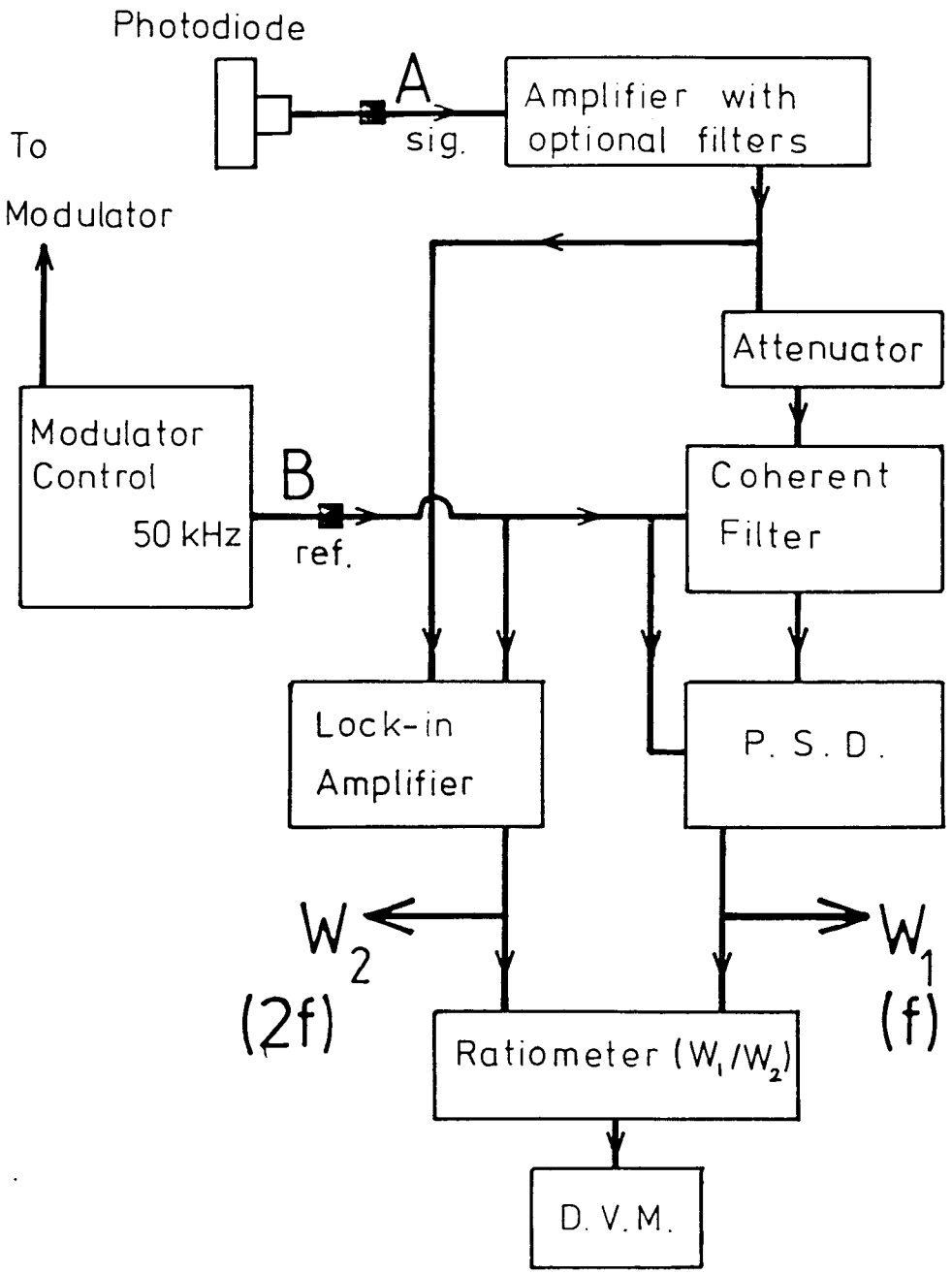
Photodiode
A
sig.
Amplifier with optional filters
To
Modulator
Attenuator
Modulator Control
50 kHz
B
ref.
Coherent Filter
Lock-in Amplifier
P. S. D.
W2
(2f)
W1
(f)
Ratiometer (W1/W2)
D. V. M.

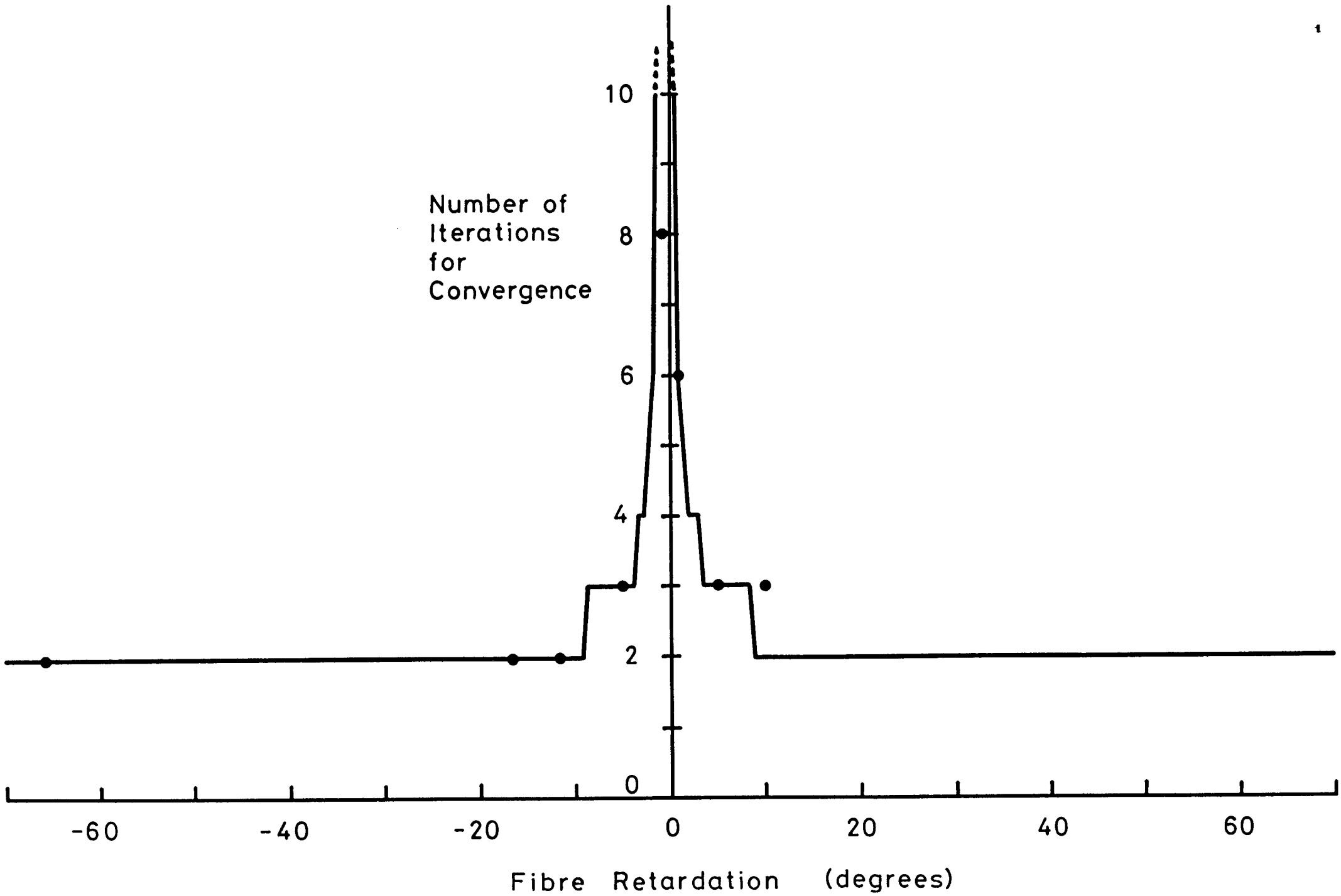
Number of Iterations for Convergence
10
8
6
4
2
0
-60
-40
-20
0
20
40
60
Fibre Retardation (degrees)

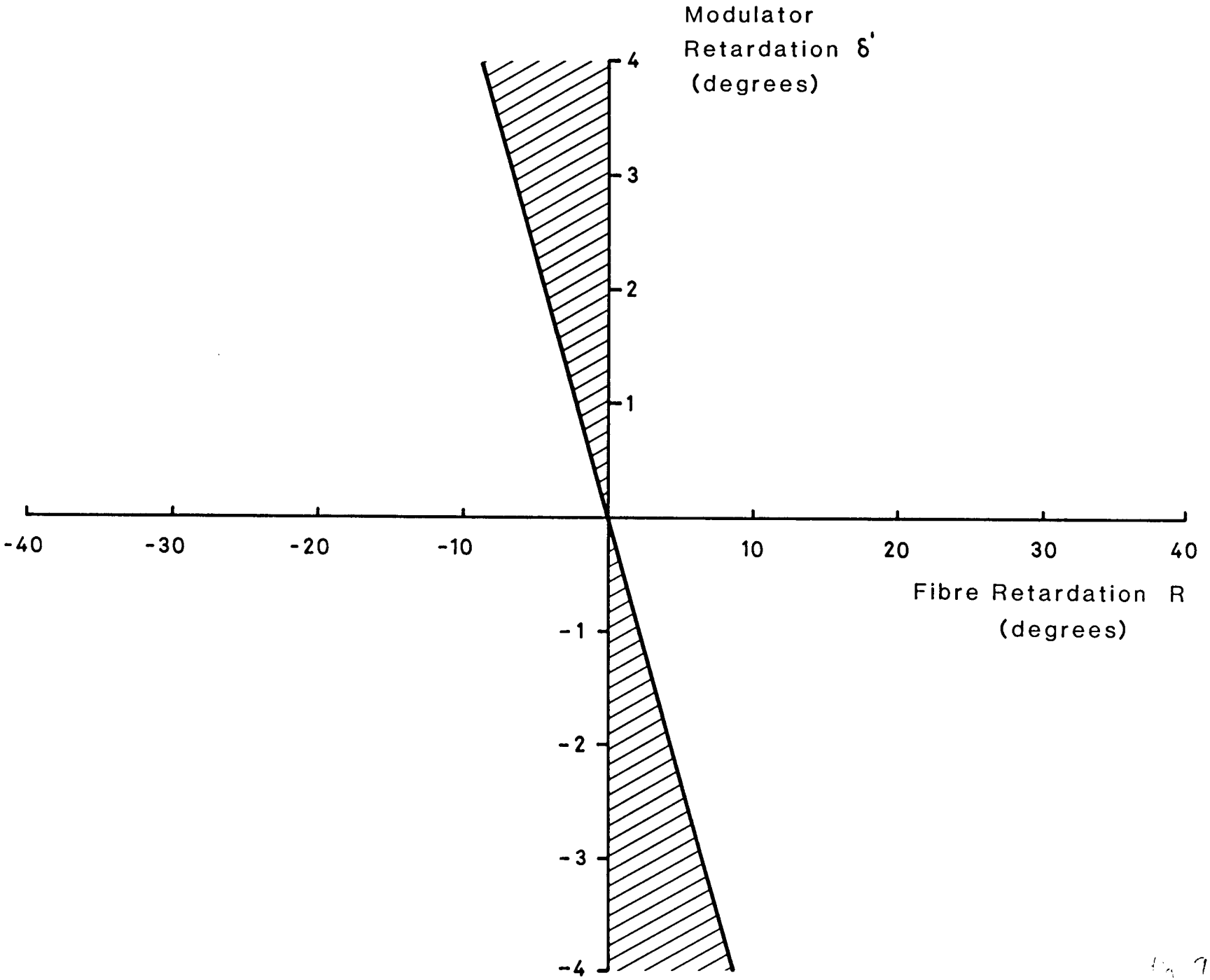
Modulator
Retardation δ'
(degrees)
4
3
2
1
-1
-2
-3
-4
-40
-30
-20
-10
10
20
30
40
Fibre Retardation R
(degrees)

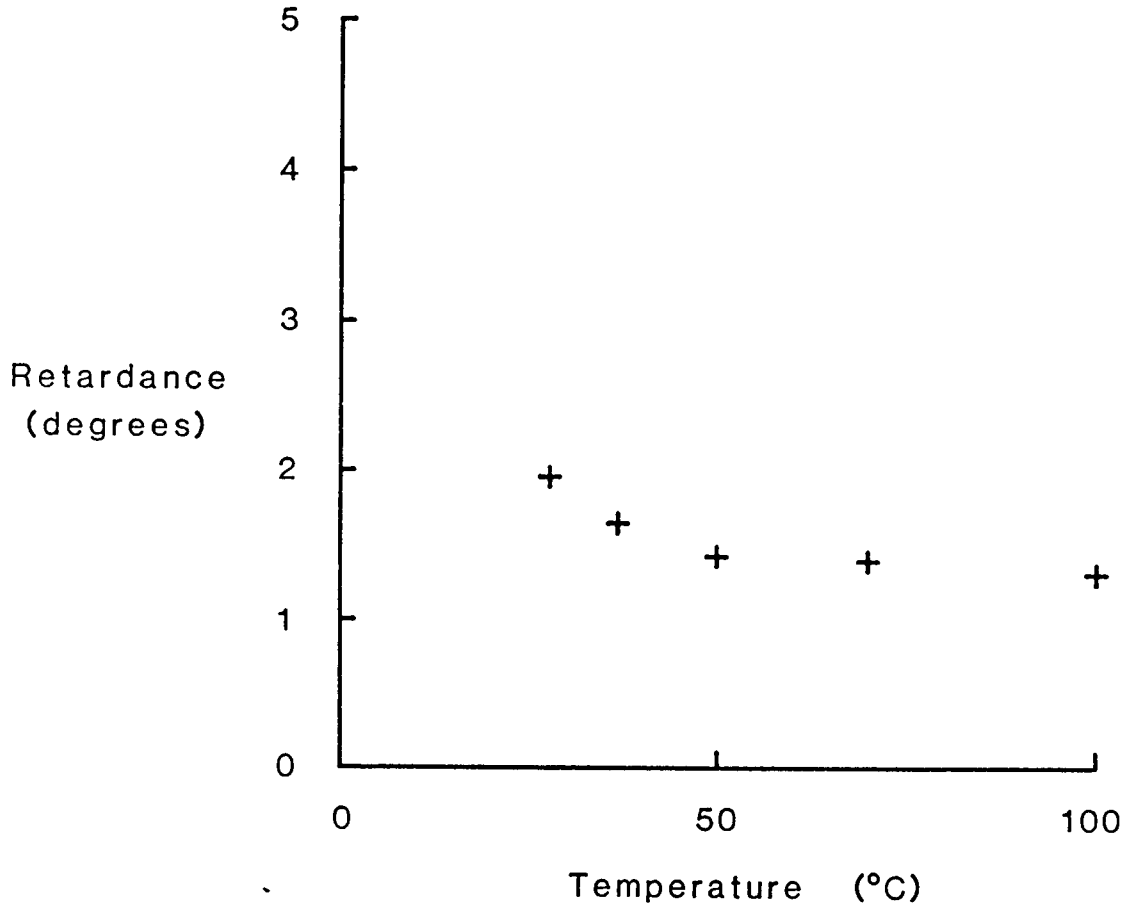

Fig 10

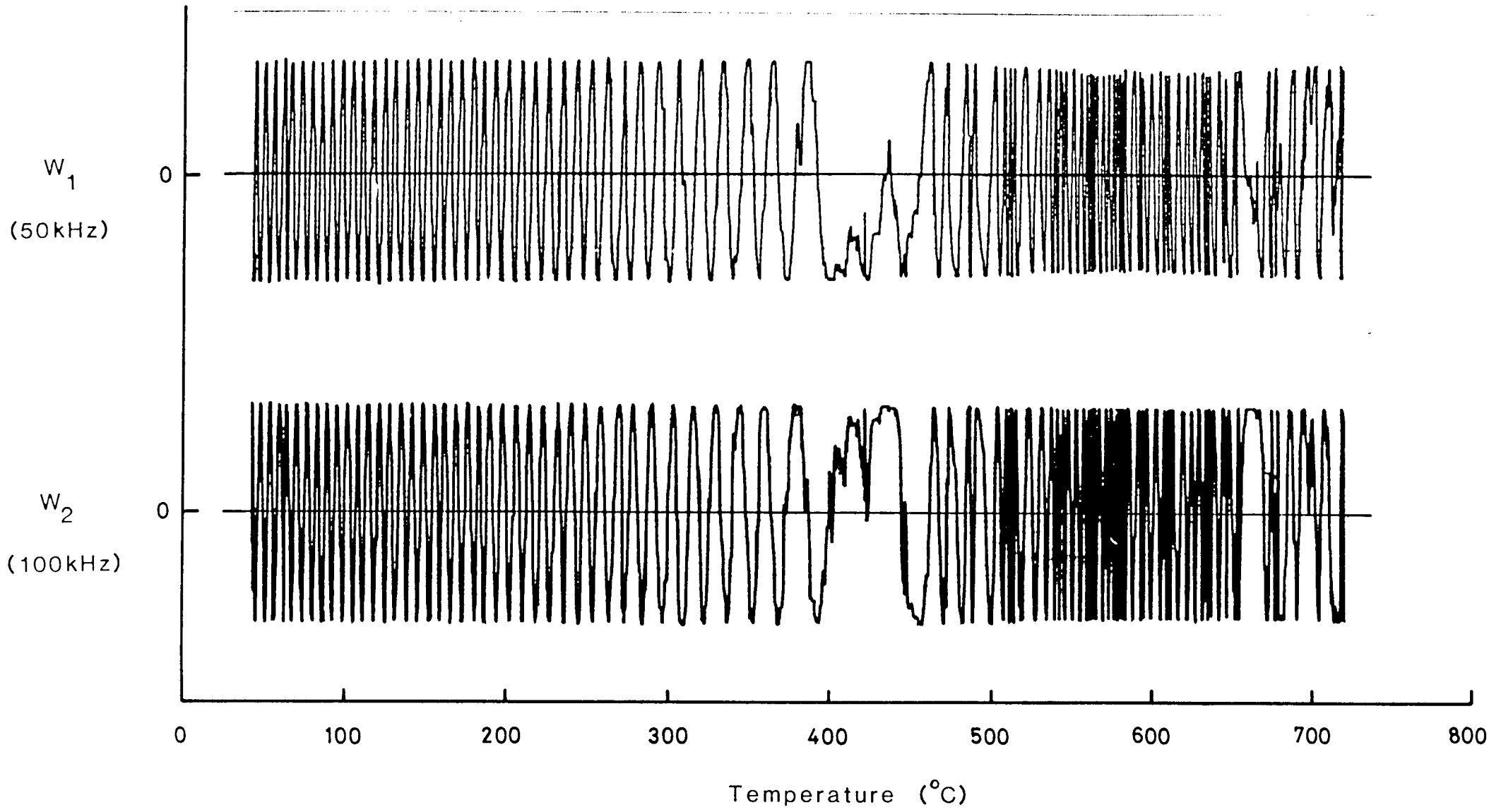
W1
(50kHz)
0
W2
(100kHz)
0
0
100
200
300
400
500
600
700
800
Temperature (°C)

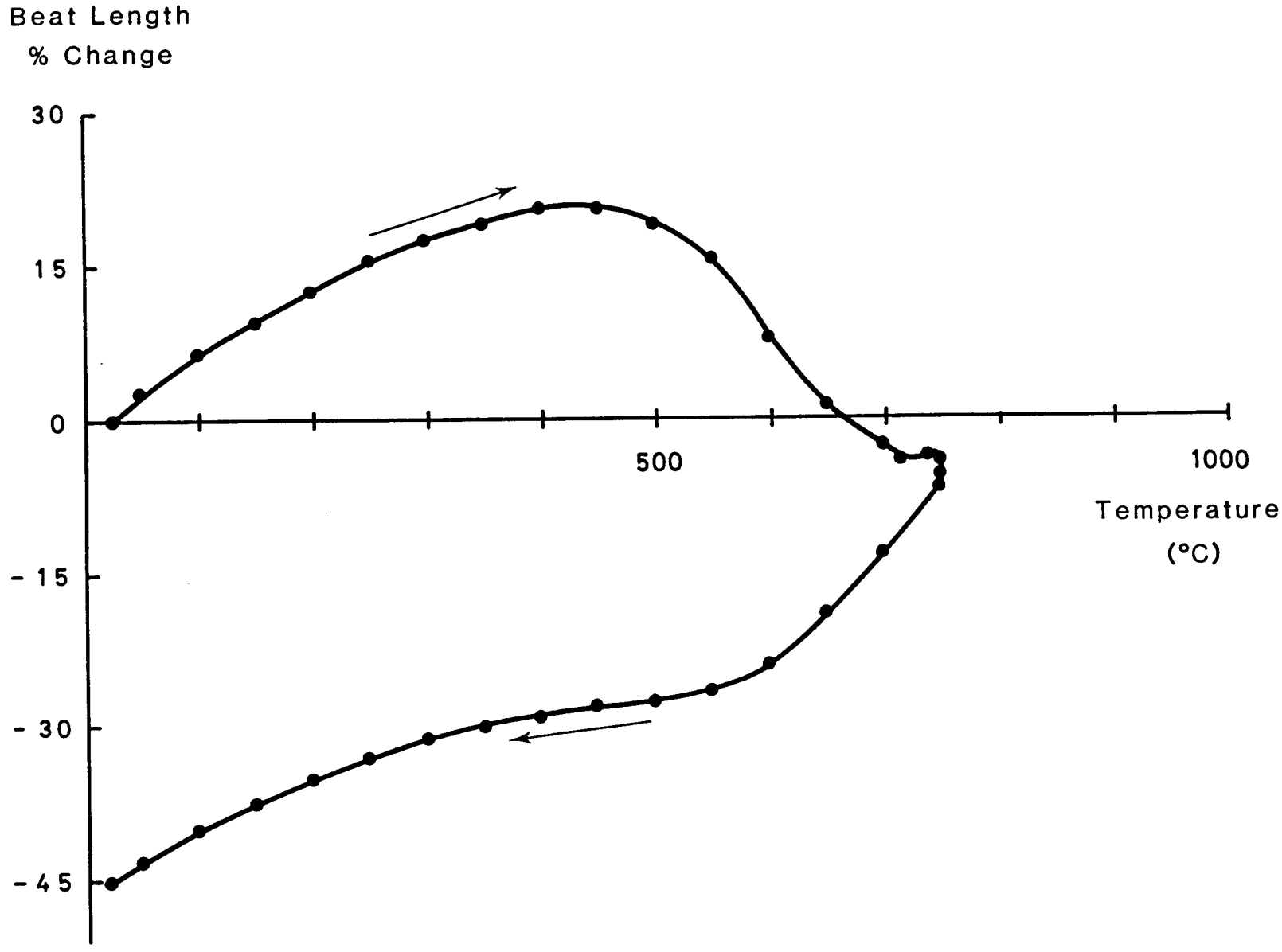

Fig 11b